3-D localization of pavers in a Computer Integrated Road Construction context

D Bouvet, G Garcia, B J Gorham, D Bétaille

3-D localization of pavers in a Computer Integrated Road Construction context

D. Bouvet[a], G. Garcia[a], B. J. Gorham[b] and D. Bétaille[c]

[a] Institut de Recherche en Communications et Cybernétique de Nantes (IRCCyN)
1 rue de la Noë, BP 92101, 44321 Nantes Cedex 3, France
gaetan.garcia@irccyn.ec-nantes.fr

[b] Industrial Metrology Research Unit (IMRU), University of East-London (UEL)
Longbridge Road, Dagenham, Essex RM8 2AS, England
b.j.gorham@uel.ac.uk

[c] Laboratoire Central des Ponts et Chaussées (LCPC)
Route de Bouaye, BP 4129, 44341 Bouguenais, France
david.betaille@lcpc.fr

Abstract

This paper presents a navigation system providing 3-D position and spatial attitude data for outdoor vehicles. Our system uses an odometer and an automatic laser theodolite, the data of which are fused using a Kalman filter. We show through different experiments carried out with the Sessyl *test station that the high accuracies required for some civil-engineering tasks are fully satisfied, provided the beacons are properly positioned.*

1 Introduction

The Computer Integrated Road Construction (CIRC) aims to share a common numerical geometrical data base from the design, through all the site operations up to the quality control of the geometry of the structure. It relies upon the following technologies: Computer Aided Design (CAD), automatic control, short-range wireless communication and real-time positioning.

In this context, a recently completed EU Brite-Euram research project resulted in the successful development of new control and monitoring systems for road construction equipment, to be integrated into compactors (CIRCOM) and asphalt pavers (CIRPAV) as target applications [11].

Designing an automatic process that takes the initial CAD road design and translates this into a finished product, a road built to specification, requires the provision in real-time of position and attitude information for the different machines.

On compactors, an integrated system has been developed, using dead-reckoning sensors (Doppler radar, encoder and fibre-optic gyrometer) in addition to RTK GPS, unable to work continuously when alone (particularly under the bridges). A maximum deviation of 20 cm was obtained for 100 m long masks, which meets the CIRCOM specifications [8].

On asphalt pavers, RTK GPS precision was not sufficient and IMRU developed the measurement system Laserguide, designed to meet the project specification for the spatial parameters of the paver, namely ± 30 mm in x and y, ± 10 mm in z, and $\pm 0.1^\circ$ in pitch and roll.

The paper describes the additional developments that have been performed by IRCCyN, UEL and LCPC outside the framework of CIRC, in terms of localization algorithm. It is organised as follows. The Laserguide is described in section 2. Section 3 details the choice of representation of the mobile robot 3-D posture and proposes a 3-D evolution model. The modelling of the Laserguide measurements is also presented and the resulting localisation algorithm based on Extended Kalman Filtering (EKF) is derived. Problematic situations for the initial localization by theodolite are also presented. Results of tests carried out on a mobile platform are given in section 4 and are followed by conclusions in section 5.

2 The Laserguide

2.1 Existing solutions

Some possible, currently available, solutions to the problem of providing the necessary position and attitude information for the paver were considered initially. The first of these was GPS, and after some careful study, was ultimately rejected for the following reasons. The cost of establishing a Base Station, together with its high speed and often long-range radio link, as well as a minimum of one mobile receiver per vehicle, is often significant in relation to the actual cost of the vehicles themselves. Moreover, the system is dependent on the field of view of its receivers and this seldom can be guaranteed without interruption during a day's operations. In some circumstances that prevail, in Scandinavian countries for instance, where a roadway is to be constructed through forests or in cuttings, the satellite receivers are unable to detect sufficient satellites to obtain a fix over periods of several hours.

In addition to shadow zones where insufficient signals are received, multi-path errors can be significant in the environment of a work-site. These effects allow measurements data to be produced but the noise factor associated with the position data can become unacceptably high. Furthermore, and following a loss of lock between an individual mobile receiver and the Base Station, there can be a significant delay in restoring the full communication ability of the system. This is particularly relevant to operation of a paver which cannot pause whilst guidance information is interrupted.

Practical accuracies quoted for 3-D co-ordinates from a GPS receiver in this dynamic mode are between ± 5 and ± 10 mm for both x and y, and between ± 20 and ± 30 mm in the z parameter (height) – well short of the requirements of the new control systems for paving. However, these can be improved under certain conditions [10]. In addition, information concerning vehicle tilts and heading can be obtained, albeit of less than the required accuracy, by using a pair of spaced GPS receivers fixed to opposite corners of the vehicle.

The other system considered for automatic guidance of the paver is a Robotic Total Station (RTS) [1]. The attainable dynamic accuracies of the respective commercial systems are very similar. They are generally equivalent to a standard error in direction of ± 5 arc seconds, and in distance measured, to ± 6 mm. The only mode of use for RTS instruments in vehicle guidance so far reported is that where the instrument is established in a fixed position at the rear and to one side of the vehicle. The measurements are automatically undertaken to a single target prism rigidly fixed to part of the vehicle chassis, or in the case of a road paver, to part of the 'screed'. Both update rate for the measurements and dynamic accuracy requirements for x, y and z are easily met.

However, use of a single RTS instrument cannot at present provide real-time spatial attitude information for a moving road paver. Accordingly, it is common to employ either on-board sensors for heading and tilts or to use two targets on the vehicle, for example, one back right and the other front left, and consequently operate two RTS instruments simultaneously [2]. A further necessary feature of use is provision of a radio data link to communicate the measurement information from instrument to vehicle.

In practice, a RTS determines its own position and orientation in relation to the local site survey reference system before finding and locking on automatically to the vehicle target prism. Thereafter, the prism is tracked as the vehicle moves and the xyz co-ordinate information for the target is transmitted regularly to the vehicle computer for onboard control or display. Clearly, in this process, the RTS is dedicated to only one vehicle at a time. Further, the intrinsic accuracy limit in the instrument measures of vertical angles, for this single-ended measurement system operating in site conditions, ensures that a required accuracy of ± 5 mm in target height cannot be achieved beyond about 250 metres range.

2.2 A new approach

In view of these shortcomings of the current systems, and more particularly, since there appears to be limited scope for their improvement in the context of site-vehicle guidance, it was decided to develop a fundamentally different approach. The technique chosen was one based on an automatic laser theodolite, developed by, and first given a public demonstration in 1983 as an RTS in, what is now the University of East London. Earliest publication of the main features of this instrument is given in [3, 4]. Since then, the technology has been developed in applications to surveying, robot calibration and automatic tunnel guidance. A features summary of LASERGUIDE is given below.

The theodolite operates by continuous scanning of a compound laser beam comprising a pair of mutually inclined fans. The rotation of the beam is monitored internally by a single electronic angle encoder. When either of the fan beam components strikes an elec-

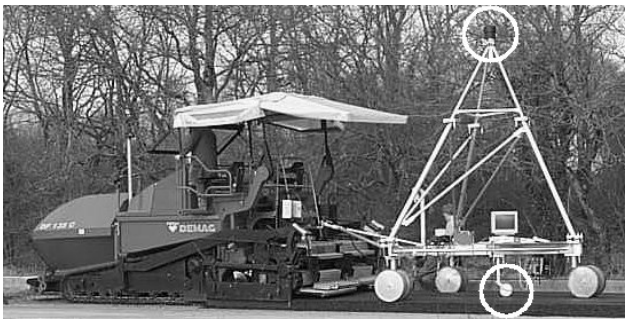

Figure 1: A CIRPAV demonstration: the LASERGUIDE is mounted on a trolley drawn by the asphalt paver and equipped with an encoder wheel

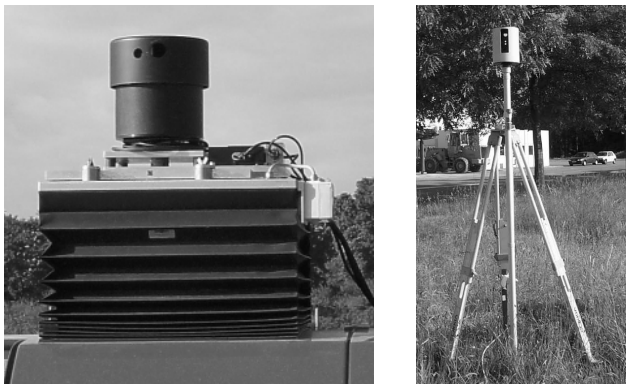

Figure 2: The LASERGUIDE mounted on station SESSYL and one of the robotic beacons

tronic or passive retro-reflecting target, the instantaneous reading of the encoder is latched and recorded.

There is almost no limit to the number of targets whose directions can be measured per sweep of the laser beams. For site vehicle guidance, the sweep rate is 1 or 2 Hz, and for short-range position monitoring, it can be increased to some 30 Hz. The repeatable pointing accuracy per target is between 1 and 2 arc seconds for ranges up to 100 metres in good optical sight conditions, and in this respect, compares favourably with current performance of commercial RTS instruments [5].

When the first prototype system (LASERGUIDE MK I) was developed for paver guidance, the instrument was designed to be set up at the rear and to one side of the paver as for a conventional RTS. A fixed array of photocells constituted the staff unit and was mounted on the rear of the paver. An infra-red laser pulse transmitter was used to convey every sixth angular minute marker from the instrument encoder to the staff. Time interpolation at the staff enabled a computation of the respective direction vectors to an accuracy of 1 to 2 arc seconds. The six spatial parameters of the staff were computed at the staff, and these could be translated into spatial parameters for the supporting paver. The first phase of testing of LASERGUIDE MK I used the SESSYL facility at LCPC and took place during May 1998.

However, although providing more real-time spatial information than a conventional RTS, and delivering data of comparable accuracy, this configuration also suffered from the same practical disadvantage; namely, guidance was lost while the instrument was moved forward to a new set-up. Obviously, the use of two instruments operating in leap-frog fashion does provide a solution, but it is a crude and expensive one.

Accordingly, and in order better to exploit the capability of a LASERGUIDE system to measure to multiple targets in a short space of time, it was decided to mount the instrument directly on the vehicle itself or on a towed sled or trolley (LASERGUIDE MK II; see figure 1). Here, the electronic targets of the staff are replaced by a number of local survey beacons distributed along the edges of the site, a configuration which provides uninterrupted real-time vehicle guidance.

The beacons are established along a line of known points along both sides of the road trajectory. Their positions must be known accurately in terms of site global x, y and z co-ordinates although they do not have to be set out in a strictly regular spatial pattern. The scanning LASERGUIDE measures the directions of each of the beacons struck by its beams, and this data is used to compute the instrument position and attitude. The minimum number of beacons necessary to provide this information is three, although a redundancy of at least one beacon becomes a practical requirement.

These beacons, which have been developed for use with LASERGUIDE, are robotic optical transponders. They seek and maintain their pointing towards the scanning laser instrument on the paver and, each time an integral photocell is struck by one of the sweeping fan beams, they transmit a very short optical pulse back towards the instrument. These 'reflections' latch the single integral angle encoder used to generate the six spatial parameters of the instrument and correspondingly of its underlying road surface.

The LASERGUIDE instrument and one of its four associated robotic beacons provided for the field tests at LCPC in November 1999 are shown in figure 2.

3 3-D localization by EKF

From the measured directions of the beacons struck by the laser beams, it is possible to compute by spatial resection the LASERGUIDE and vehicle 3-D postures. As we will see in subsection 3.4, this approach is used to evaluate the initial position and attitude of the asphalt paver. But for real-time positioning, an Extended Kalman Filter is used. Indeed, fusing the LASERGUIDE angles with the measurements of an additional encoder wheel presents several advantages. First, it allows to maintain an estimation of the vehicle 3-D posture even when angle measurements are unavailable (either because the beacons are temporary masked by another vehicle, or because the theodolite measurements are erroneous). Secondly, it is possible to take into account the angles issued by the theodolite one at a time contrary to quasi-static approaches where several measurements are used simultaneously, as if corresponding to a single position and attitude of the paver. And finally, although the LASERGUIDE scanning rate is 1 Hz, integrating measurements of the complementary sensor allows to provide position and attitude data at a higher frequency.

3.1 Definition of the 3-D pose and kinematic model of the vehicle

Six independent variables are generally required to describe the 3-D posture (position and attitude) of a vehicle. For our application, the position is defined by the co-ordinates (x, y, z) of the centre M of the encoder wheel in the reference frame R_0, and for the attitude, the roll-pitch-heading angles have been chosen. As a consequence, the 3-D posture is defined by:

$$\mathbf{x} = [x, y, z, R, P, H]^t \tag{1}$$

From this choice of representation a kinematic model adapted to the asphalt pavers was derived. Since these are very slow machines (about 10 cm/s) working on smooth terrain with very progressive gradient variations, the vehicle is assumed to move between instants t_{i-1} and t_i on an inclined plane defined by the roll and pitch angles R_{i-1} and P_{i-1}. The movement on this plane is considered as an elementary translation δ followed by an elementary rotation of speed ω. Since an unique encoder wheel is used, only δ is measured and ω is estimated by EKF. Denoting T_s the sampling

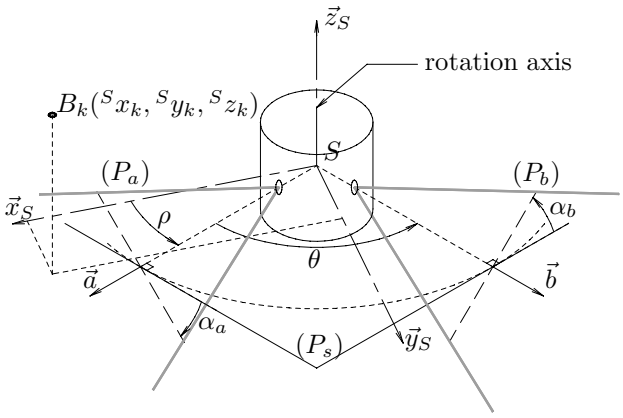

Figure 3: Sensor modelling

period, the resulting evolution model is given by:

$$\begin{aligned}
x_i &= x_{i-1} + \delta_i \cos(P_{i-1}) \cos(H_{i-1}) \\
y_i &= y_{i-1} + \delta_i [\cos(R_{i-1}) \sin(H_{i-1}) + \dots \\
&\quad \cos(H_{i-1}) \sin(P_{i-1}) \sin(R_{i-1})] \\
z_i &= z_{i-1} + \delta_i [\sin(H_{i-1}) \sin(R_{i-1}) + \dots \\
&\quad - \cos(H_{i-1}) \cos(R_{i-1}) \sin(P_{i-1})] \\
R_i &= R_{i-1} \\
P_i &= P_{i-1} \\
H_i &= H_{i-1} + T_s \cdot \omega_{i-1} \\
\omega_i &= \omega_{i-1}
\end{aligned} \tag{2}$$

or by the vector equation:

$$\mathbf{x}_i^a = \mathbf{f}(\mathbf{x}_{i-1}^a, u_i) \tag{3}$$

where $\mathbf{f}$ is the prediction function, u the system input (here only δ), and $\mathbf{x}^a$ the *augmented* state vector:

$$\mathbf{x}^a = [x, y, R, P, H, \omega]^t \tag{4}$$

Actually, the evolution model and the proprioceptive measurement are assumed to be corrupted by uncorrelated white Gaussian noises of mean zero and known variances:

$$\mathbf{x}_i^a = \mathbf{f}(\mathbf{x}_{i-1}^a, u_i + \beta_i) + \boldsymbol{\alpha}_i \tag{5}$$

where $\boldsymbol{\alpha}$ is the model noise of covariance matrix $\mathbf{Q}_\alpha$, and β the input noise of variance Q_β.

3.2 Laserguide modelling and observation equations

The LASERGUIDE is modelled as shown on figure 3. The fan-shaped laser beams are denoted (P_a) and (P_b). The sensor centre S is given by the intersection of (P_a) and (P_b) with the rotation axis $\vec{z}_S$. An

encoder allows to measure the rotation angle ρ with a precision of 1 arc second.

α_a and α_b are the tilt angles of half-planes (P_a) and (P_b). The plane containing S and orthogonal to the rotation axis is denoted (P_c). Vector $\vec{a}$ is defined by $(P_s)\cap(P_a) = [S, \vec{a})$ and vector $\vec{b}$ by $(P_s)\cap(P_b) = [S, \vec{b})$. Angle θ is given by $\theta = \angle(\vec{a}S\vec{b})$ and vector $\vec{x}_S$ is such that $\vec{x}_S = \vec{a}$ when $\rho = 0$. The frame F_S associated with the sensor is given by $(S, \vec{x}_S, \vec{z}_S \wedge \vec{x}_S, \vec{z}_S)$.

Each laser beam emitter is associated with an IR receiver oriented along axis $\vec{a}$ (resp. $\vec{b}$). Thus, whenever the LASERGUIDE receives a pulse from a beacon, it is possible to know which laser beam has struck the target by checking which receiver has detected the signal. The corresponding encoder reading is denoted ρ^a or ρ^b.

When the laser beams strike beacon B_k, the corresponding angular measurements $\rho^{a,k}$ and $\rho^{b,k}$ are given by:

$$\begin{array}{rcl} s^{a,k} & = & -{}^S x_k\, {}^S z_k \cot(\alpha_a) + \ldots \\ & & {}^S y_k \sqrt{({}^S x_k^2 + {}^S y_k^2) - {}^S z_k^2 \cot(\alpha_a)^2} \\ c^{a,k} & = & {}^S y_k\, {}^S z_k \cot(\alpha_a) + \ldots \\ & & {}^S x_k \sqrt{({}^S x_k^2 + {}^S y_k^2) - {}^S z_k^2 \cot(\alpha_a)^2} \\ \rho^{a,k} & = & \arctan2(s^{a,k}, c^{a,k}) \end{array} \quad (6)$$

$$\begin{array}{rcl} s^{b,k} & = & -{}^S x_k\, {}^S z_k \cot(\alpha_b) + \ldots \\ & & {}^S y_k \sqrt{({}^S x_k^2 + {}^S y_k^2) - {}^S z_k^2 \cot(\alpha_b)^2} \\ c^{b,k} & = & {}^S y_k\, {}^S z_k \cot(\alpha_b) + \ldots \\ & & {}^S x_k \sqrt{({}^S x_k^2 + {}^S y_k^2) - {}^S z_k^2 \cot(\alpha_b)^2} \\ \rho^{b,k} & = & \arctan2(s^{b,k}, c^{b,k}) - \theta \end{array} \quad (7)$$

where ${}^S\mathbf{b}_k = [{}^S x_k, {}^S y_k, {}^S z_k, 1]^t$ are the homogeneous co-ordinates of beacon B_k in the sensor frame F_S. Actually, only the beacon co-ordinates ${}^0\mathbf{b}_k$ in the reference frame are known, and the homogeneous coordinates ${}^S\mathbf{b}_k$ are given by:

$${}^S\mathbf{b}_k = {}^S\mathbf{T}_M \cdot {}^M\mathbf{T}_0(\mathbf{x}) \cdot {}^0\mathbf{b}_k \quad (8)$$

The homogeneous transformation matrix ${}^S\mathbf{T}_M$ is fixed once and for all after calibration of the LASERGUIDE in the vehicle frame F_M and the homogeneous transformation matrix ${}^M\mathbf{T}_0$ depends on the 3-D posture $\mathbf{x}$ of the vehicle.

Finally, the LASERGUIDE observations at observation instant t_j can be rewritten in the following form:

$$Z_j = g^{a|b,k}(\mathbf{x}_j^a) + \gamma_j \quad (9)$$

where γ is a white Gaussian noise of mean zero and variance Q_γ, Z the system scalar output, and $g^{a|b,k}$ the observation function, the expression of which depends on the laser beam which struck the beacon and on the particular beacon struck by the beam.

3.3 Localization by Kalman filtering

Since the evolution and observation functions $\mathbf{f}$ and $g^{a|b,k}$ are nonlinear, an extended Kalman filter is used to compute the estimation $\hat{\mathbf{x}}^a$ of the augmented state vector and the associated covariance matrix $\mathbf{P}$ of the estimate error.

At each sampling period, the state estimate is predicted from the input readings δ:

$$\begin{array}{rcl} \hat{\mathbf{x}}^a_{i|i-1} & = & \mathbf{f}(\mathbf{x}^a_{i-1|i-1}, \delta_i) \\ \mathbf{P}_{i|i-1} & = & \mathbf{A}_i\, \mathbf{P}_{i-1|i-1}\, \mathbf{A}_i^t + \mathbf{B}_i\, Q_\beta\, \mathbf{B}_i^t + \mathbf{Q}_\alpha \end{array} \quad (10)$$

with the following Jacobian matrices:

$$\mathbf{A}_i = \left.\frac{\partial \mathbf{f}(\mathbf{x}^a, u)}{\partial \mathbf{x}^a}\right|_{\mathbf{x}^a = \hat{\mathbf{x}}^a_{i-1|i-1}, u_i = \delta_i} \quad (11)$$

$$\mathbf{B}_i = \left.\frac{\partial \mathbf{f}(\mathbf{x}^a, u)}{\partial u}\right|_{\mathbf{x}^a = \hat{\mathbf{x}}^a_{i-1|i-1}} \quad (12)$$

And whenever a laser beam strikes beacon B_k, this prediction is corrected as follows:

$$\begin{array}{rcl} \hat{\mathbf{x}}^a_{i|i} & = & \hat{\mathbf{x}}^a_{i|i-1} + \mathbf{K}_i \left(Z_i - g^{a|b,k}(\hat{\mathbf{x}}^a_{i|i-1}) \right) \\ \mathbf{P}_{i|i} & = & \mathbf{P}_{i|i-1} - \mathbf{K}_i\, \mathbf{C}_i^{a|b,k}\, \mathbf{P}_{i|i-1} \end{array} \quad (13)$$

where the jacobian matrix $C_i^{a|b,k}$ is given by:

$$\mathbf{C}_i^{a|b,k} = \left.\frac{\partial g^{a|b,k}(\mathbf{x}^a)}{\partial \mathbf{x}^a}\right|_{\mathbf{x}^a = \hat{\mathbf{x}}^a_{i|i-1}} \quad (14)$$

and the Kalman gain $\mathbf{K}_i$ is defined by:

$$\mathbf{K}_i = \mathbf{P}_{i|i-1}\, (\mathbf{C}_i^{a|b,k})^t \cdot \left(\mathbf{C}_i^{a|b,k}\, \mathbf{P}_{i|i-1}\, (\mathbf{C}_i^{a|b,k})^t + Q_\gamma \right)^{-1} \quad (15)$$

Actually, the IR pulses sent to the LASERGUIDE are unsigned, which means that the beacons are undistinguishable. The chi-squared distribution test provides a mean to know which target has been detected before processing the updating step.

For each beacon $B_k, k = 1 \ldots N$, the so-called Mahalanobis distance is computed as follows:

$$d_i^k = \frac{|Z_i - g^{a|b,k}(\hat{\mathbf{x}}^a_{i|i-1})|}{\sqrt{\mathbf{C}_i^{a|b,k}\, \mathbf{P}_{i|i-1}\, (\mathbf{C}_i^{a|b,k})^t + Q_\gamma}} \quad (16)$$

In the case of a linear system corrupted by white Gaussian noises of mean zero, and with a 1-dimensional innovation, the Mahalanobis distance d has a 99.7% probability to be lower than 3 [7]. Despite the fact that in our application, the system is nonlinear, we have kept this threshold. As a consequence, k such that $d_i^k < 3$ indicates which beacon has been struck by laser beam (P_a) or (P_b) at instant t_i.

The resulting localization algorithm is given by:

Initialization: $\hat{\mathbf{x}}^a_{0|0}$, $\mathbf{P}_{0|0}$
for $i = 1, 2, \ldots$ **do**
  $\delta_i \leftarrow$ odometer measurement
  $\mathbf{A}_i \leftarrow \left.\frac{\partial \mathbf{f}(\mathbf{x}^a, u)}{\partial \mathbf{x}^a}\right|_{\mathbf{x}^a = \hat{\mathbf{x}}^a_{i-1|i-1}, u=\delta_i}$
  $\mathbf{B}_i \leftarrow \left.\frac{\partial \mathbf{f}(\mathbf{x}^a, u)}{\partial u}\right|_{\mathbf{x}^a = \hat{\mathbf{x}}^a_{i-1|i-1}}$
  $\hat{\mathbf{x}}^a_{i|i-1} \leftarrow \mathbf{f}(\hat{\mathbf{x}}^a_{i-1|i-1}, \delta_i)$
  $\mathbf{P}_{i|i-1} \leftarrow \mathbf{A}_i \, \mathbf{P}_{i-1|i-1} \, \mathbf{A}_i^t + \mathbf{B}_i \, Q_\beta \, \mathbf{B}_i^t + \mathbf{Q}_\alpha$
  $\tilde{\mathbf{x}}^a \leftarrow \hat{\mathbf{x}}^a_{i|i-1}$
  $\tilde{\mathbf{P}} \leftarrow \mathbf{P}_{i|i-1}$
  for each angular measurement Z performed between t_{i-1} and t_i **do**
    for each beacon B_k **do**
      $\mathbf{C}_i^{a|b,k} \leftarrow \left.\frac{\partial g^{a|b,k}(\mathbf{x}^a)}{\partial \mathbf{x}^a}\right|_{\mathbf{x}^a = \tilde{\mathbf{x}}^a}$
      $d_i^k \leftarrow \frac{|Z(j) - g^{a|b,k}(\tilde{\mathbf{x}}^a)|}{\sqrt{\mathbf{C}_i^{a|b,k} \, \tilde{\mathbf{P}} \, (\mathbf{C}_i^{a|b,k})^t + Q_\gamma}}$
    end for
    if $\min(d_i^k) < 3$ **then**
      $l \leftarrow \arg\min d_i^k$
      $\mathbf{K}_i \leftarrow \tilde{\mathbf{P}} \, (\mathbf{C}_i^{a|b,l})^t \left(\mathbf{C}_i^{a|b,l} \, \tilde{\mathbf{P}} \, (\mathbf{C}_i^{a|b,l})^t + Q_\gamma \right)^{-1}$
      $\tilde{\mathbf{x}}^a \leftarrow \tilde{\mathbf{x}}^a + \mathbf{K}(i)[Z(i) - g^{a|b,l}(\tilde{\mathbf{x}}^a)]$
      $\tilde{\mathbf{P}} \leftarrow \tilde{\mathbf{P}} - \mathbf{K}(i) \, \mathbf{C}_i^{a|b,l} \, \tilde{\mathbf{P}}$
    end if
  end for
  $\hat{\mathbf{x}}^a_{i|i} \leftarrow \tilde{\mathbf{x}}^a$
  $\mathbf{P}_{i|i} \leftarrow \tilde{\mathbf{P}}$
end for

Algorithm 1: 3-D localization with unsigned beacons by EKF

3.4 Localization initialization

To work properly, the EKF requires a good estimation $\hat{\mathbf{x}}^a_{0|0}$ of the initial state vector. Since the paver is assumed to be motionless when starting its work, we have $\hat{\omega}_{0|0} = 0$ rad/s.

The initial 3-D posture $\hat{\mathbf{x}}_{0|0}$ is computed from the full direction vector (both horizontal and vertical directions) to three non aligned beacons as follows.

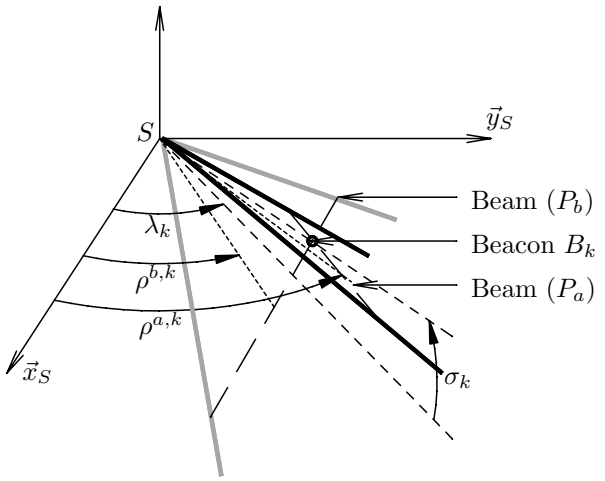

Figure 4: Azimuth and elevation angles of beacon B_k and corresponding LASERGUIDE angular measures

When motionless, the LASERGUIDE is equivalent to a theodolite, i.e. an instrument which can measure the azimuth and elevation angles of a given target. These angles are computed from the LASERGUIDE measures $\rho^{a,k}$ and $\rho^{b,k}$ as follows:

$$\lambda_k = \rho^{a,k} + \arctan\left(\frac{\frac{\tan(\alpha_a)}{\tan(\alpha_b)} \sin(\rho^{a,k} - \rho^{b,k} - \theta)}{1 - \frac{\tan(\alpha_a)}{\tan(\alpha_b)} \cos(\rho^{a,k} - \rho^{b,k} - \theta)} \right)$$
$$\sigma_k = \arctan\left(\tan(\alpha_a) \cdot \sin(\lambda_k - \rho^{a,k})\right) \quad (17)$$

If one tries to solve the localization problem directly by writing the equations that involve the position and attitude of the vehicle, one obtains a complex system of six nonlinear equations with six unknowns. Actually, as shown in [6], it is possible to reduce this system to a problem with 3 unknowns by introducing the distances between the sensor and the beacons as new variables.

Let r_k be the distance from the origin of the sensor frame S to beacon B_k. The co-ordinates of B_k in the sensor frame are given by:

$$\begin{aligned} {}^S x_k &= r_k \cos(\lambda_k) \cos(\sigma_k) \\ {}^S y_k &= r_k \sin(\lambda_k) \cos(\sigma_k) \\ {}^S z_k &= r_k \sin(\sigma_k) \end{aligned} \quad (18)$$

By writing the (known) distances d_{ij} between beacons B_i and B_j, three equations of the following form are obtained:

$$\alpha_{ij} = r_i / r_j + r_j / r_i - d_{ij}^2 / (r_i \cdot r_j) \quad (19)$$

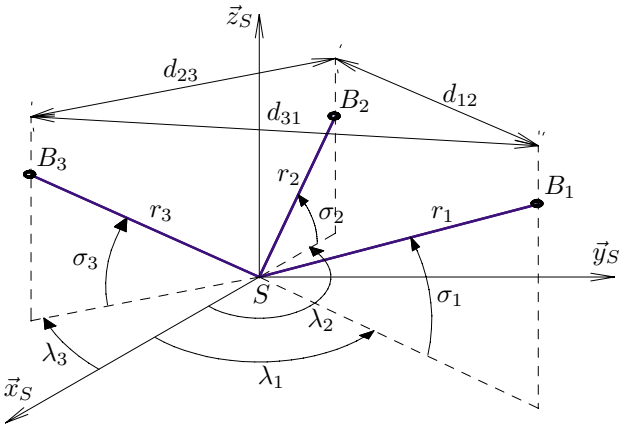

Figure 5: Variables involved in the computation of the initial 3-D posture

where

$$\begin{aligned}\alpha_{ij} = \; & 2(\cos(\sigma_i)\cos(\lambda_i)\cos(\sigma_j)\cos(\lambda_j) + \dots \\ & \cos(\sigma_i)\sin(\lambda_i)\cos(\sigma_j)\sin(\lambda_j) + \sin(\sigma_i)\sin(\sigma_j))\end{aligned} \tag{20}$$

Finding the values r_k provides the co-ordinates of the beacons in the sensor frame. If one defines a frame F_B associated with the three non aligned beacons, one can compute the homogeneous transformation ${}^S\mathbf{T}_B$. Knowing ${}^0\mathbf{T}_B$ and ${}^M\mathbf{T}_S$, it is easy to obtain the homogeneous transformation matrix ${}^0\mathbf{T}_M$ and hence, the spatial position and orientation of the vehicle in the work site frame:

$${}^0\mathbf{T}_M(\mathbf{x}) = {}^0\mathbf{T}_B \cdot {}^S\mathbf{T}_B^{-1} \cdot {}^S\mathbf{T}_M \tag{21}$$

As a consequence, the whole problem lies in finding the good association beacons-angles (recall that the beacons are unsigned) and in determining the proper distances r_1, r_2 and r_3. The algorithm dealing with this issue is not discussed here, but it works provided the theodolite is not stopped on the cylinder generated by the circle passing by the three beacons and normal to the plane containing these beacons. This can be shown by studying the observability of the following system, defined from equation (20):

$$\boldsymbol{\alpha} = \mathbf{h}(\mathbf{r}) \tag{22}$$

where the system output is $\boldsymbol{\alpha} = [\alpha_{12}, \alpha_{23}, \alpha_{31}]^t$ and the state vector is $\mathbf{r} = [r_1, r_2, r_3]^t$.

The property of observability for a dynamical system is related to the possibility to reconstruct the state information given the inputs and outputs of the system. In the specific case of static localisation using theodolite, the problem is simple to study, since the dimension of the output vector equals the dimension of the state vector $\mathbf{r}$. In this case, one simply finds the non observable situations by checking the rank of the jacobian matrix $\left[\frac{\partial \mathbf{h}}{\partial \mathbf{r}}\right]$. Its determinant is given by the following expression:

$$\Delta = \begin{vmatrix} \frac{r_1^2 - r_2^2 + d_{12}^2}{r_1^2 r_2} & \frac{r_2^2 - r_1^2 + d_{12}^2}{r_1 r_2^2} & 0 \\ 0 & \frac{r_2^2 - r_3^2 + d_{23}^2}{r_2^2 r_3} & \frac{r_3^2 - r_2^2 + d_{23}^2}{r_2 r_3^2} \\ \frac{r_1^2 - r_3^2 + d_{31}^2}{r_1^2 r_3} & 0 & \frac{r_3^2 - r_1^2 + d_{31}^2}{r_3 r_1^2} \end{vmatrix} \tag{23}$$

In a frame denoted F_{123}, the origin of which is the centre of the circle of radius R passing through the three beacons, and the z axis of which is orthogonal to the plane containing these beacons, the homogeneous co-ordinates of beacon B_k and the theodolite centre S are given by:

$$\begin{aligned} {}^{123}\mathbf{b}_k &= [R\cos(\theta_k), R\sin(\theta_k), 0, 1]^t & (24) \\ {}^{123}\mathbf{s} &= [\rho\cos(\theta), \rho\sin(\theta), h, 1]^t & (25) \end{aligned}$$

Hence, we have:

$$\begin{aligned} r_i^2 &= R^2 + \rho^2 + h^2 - 2R\rho\cos(\theta_i - \theta) & (26) \\ d_{ij}^2 &= 2R^2(1 - \cos(\theta_i - \theta_j)) & (27) \end{aligned}$$

With this choice of representation, the numerator of determinant Δ is given after simplification by:

$$(R^2 - \rho^2)\left(\sin(\theta_1 - \theta_2) + \sin(\theta_2 - \theta_3) + \sin(\theta_3 - \theta_1)\right)^2 \tag{28}$$

which means that $\Delta = 0 \Leftrightarrow \rho = R$, since $\theta_1 \neq \theta_2$, $\theta_2 \neq \theta_3$ and $\theta_3 \neq \theta_1$.

As a consequence, the whole set of non-observable positions with a theodolite is contained in the cylinder generated by the circle passing through the three beacons and orthogonal to the plane containing these beacons, which means that near this cylinder, the accuracy of the estimation of the initial position falls drastically.

4 Experimental results

4.1 The Sessyl station

To evaluate the LASERGUIDE performances, we have used the SESSYL station, which is the localization systems test and research facility of the Laboratoire Central des Ponts et Chaussées. Its main objective is to support the research work and localization systems assessments carried out in the field of site robotics and

Figure 6: The SESSYL station

dynamic positioning of construction equipment. Most of land positioning systems, either static or dynamic, can be evaluated on this bench:

- GPS receivers, absolute, differential and Real-Time Kinematic,
- radio positioning systems using ground beacons,
- optical systems using laser triangulation, such as the LASERGUIDE,
- levelling systems using laser plane, etc.

It consists of a closed track composed of a metal rail fixed upon a concrete wall and a mobile carriage moving on it. The upper part of the carriage is a platform which can be controlled in height, pitch and roll by three jacks and which supports the tested localization system.

The computation of the SESSYL reference trajectory requires a static calibration. To this end, a SOKKIA NET 2 theodolite was used to perform a static survey of 300 positions of the carriage around the track. The curvilinear abscissa of each station (distance travelled by SESSYL along the track from the origin of the reference frame F_0) was also computed using the measurements of the theodolite.

During a test, the following data are stored with a frequency of 64 Hz:

- the position of the platform relative to the carriage (with three position transducers),
- the attitude of the platform (directly measured with two inclinometers),

Degree of freedom	Amplitude	Accuracy ($\pm 2\sigma$)
x	81 m	± 5 mm
y	16 m	± 5 mm
z	30 cm	± 2 mm
R	6°	$\pm 0.07°$
P	6°	$\pm 0.05°$
H	360°	$\pm 0.1°$

Table 1: Movement amplitude and accuracy of the SESSYL station

- the distance travelled by SESSYL along the track (with an encoder, the resolution of which is 3 mm, and which is corrected every 10 to 15 m),
- the time (with one millisecond resolution).

Since the trajectory followed by the carriage is perfectly known, it is possible to reconstruct at each sampling period the complete 3-D posture of the platform in the reference frame F_0. Table 1 summarizes the main features of SESSYL. For further details on this station, the reader is referred to [9].

4.2 Tests and results

Although only three beacons are needed to localize the mobile platform, a fourth one has been settled (see figure 7) and it is used in the positioning computations. Several tests have been carried out. The data issued by all sensors are recorded and post-processed so as to compare the reference 3-D posture of the SESSYL platform with its estimation by our 3-D localization algorithm. The movements of the mobile platform have been programmed as follows:

- tests 1, 2 and 3: one or two complete laps at constant speed (10 cm/s) without height, gradient and cross-fall variations,
- test 4: one complete lap without height, gradient and cross-fall variations, but with numerous stops, so as to simulate the real motions of a paver on site,
- tests 5 and 6: one complete lap at constant speed with variations of the cross-fall angle,
- tests 7 and 8: variations of height and gradient angle. The platform movements are programmed so as to simulate a vehicle moving on a road with a variable slope.

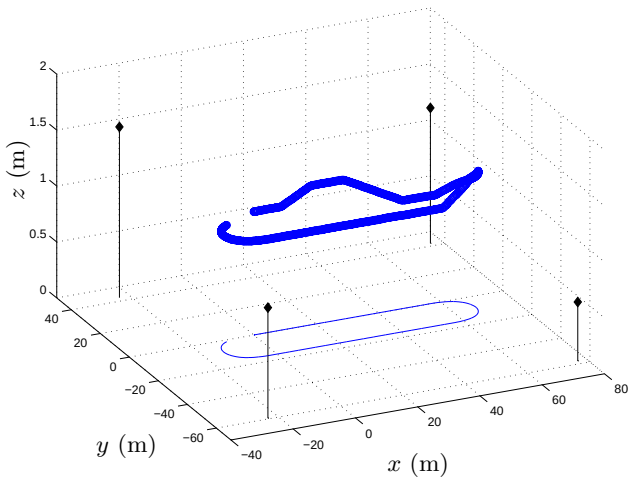

Figure 7: 3-D position of the SESSYL platform and location of the four beacons for a test with height and gradient variations

The first validation is to verify that the platform rotation speed ω is properly estimated by the EKF. The comparison of the estimate $\hat{\omega}$ with the output of a fibre-optic gyro fixed on SESSYL shows that both speeds are almost identical and confirms that, with the LASERGUIDE, an encoder wheel is sufficient to evaluate the 3-D posture of asphalt pavers.

The second validation consists in seeing to what extent the positioning requirements defined in the framework of the CIRC project are satisfied. To this end, the following percentages have been calculated:

- estimations within the planimetric tolerance: $\sqrt{(x_{Sessyl} - \hat{x})^2 + (y_{Sessyl} - \hat{y})^2} \leq 3$ cm,
- estimations within the altimetric tolerance: $|z_{Sessyl} - \hat{z}| \leq 1$ cm,
- estimations within the R-positioning tolerance: $|R_{Sessyl} - \hat{R}| \leq 0.1°$,
- estimations within the P-positioning tolerance: $|P_{Sessyl} - \hat{P}| \leq 0.1°$,
- fully satisfying position estimations,
- fully satisfying attitude estimations,
- fully satisfying posture estimations.

Table 2 reports the positioning accuracy of the LASERGUIDE. Tests 4 and 8 excepted, more than 95% of the estimated 3-D postures satisfy the requirements defined by the end-users of a localization system for asphalt pavers.

Test	xy	z	R	P	xyz	RP	all
1	99.7	99.6	98.5	99.6	99.4	98.1	97.7
2	99.7	100	98.7	99.9	99.7	98.6	98.4
3	97.8	100	99.1	99.9	97.8	99.0	96.8
4	99.6	99.8	98.4	95.9	99.4	94.5	94.3
5	99.3	99.7	98.5	99.3	99.1	97.9	97.4
6	96,9	99.1	98.8	99.8	96.0	98.8	95.0
7	99.7	98.4	99.7	98.1	98.3	97.9	96.9
8	96.0	99.9	98.9	99.2	95.9	98.3	94.8

Table 2: Percentages of estimations within the fixed tolerances

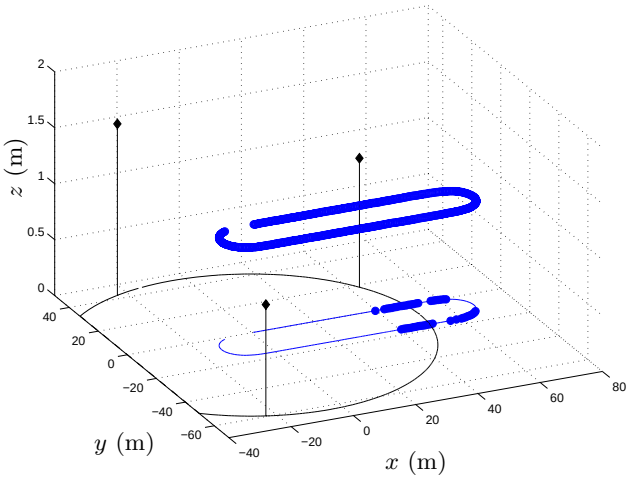

Figure 8: 3-D position of the SESSYL platform and location of the three beacons for the additional test. The areas where the planimetric error exceeds 3 cm are visible in the xy plane.

Yet, these performances can be drastically reduced in particular conditions. The test presented in the following subsection illustrates this phenomenon.

4.3 Additional test

Our concern was to evaluate the EKF behaviour when the asphalt paver moves through the cylinder problematic for the initial localization. To this end, three beacons have been positioned so that the resulting cylinder intersects the SESSYL track. As figure 8 testifies, the positioning accuracy drops when the carriage approaches the cylinder and the LASERGUIDE performances are strongly degraded (see table 3).

To avoid such a phenomenon, one will have to make sure that four beacons are always visible for the LASERGUIDE and that these beacons do not belong to the same circle.

Test	xy	z	R	P	xyz	RP	all
9	80.3	99.9	98.9	99.9	80.3	98.8	79.2

Table 3: Percentages of estimations within the fixed tolerances for the additional test

5 Conclusion

In order to determine precisely and in real-time the 3-D co-ordinates and spatial attitude of asphalt pavers, a localisation system, which fuses by Kalman filtering measurements issued by an odometer and an automatic laser theodolite, is proposed.

Through the different experiments carried out with the evaluation station SESSYL, it has been shown that a second proprioceptive sensor was not necessary to evaluate the rotation speed of the machine in the rolling plane, since its estimation by the extended Kalman filter precisely corresponds to the outputs of a fibre-optic gyro fixed on the station.

Moreover, with this navigation algorithm, 95% of the estimated postures meet the accuracy requirements, namely ± 3 cm in x and y, ± 1 cm in z and $\pm 0.1°$ in pitch and roll. As a comparison, the positioning error of the previous method, based on quasi static 3-D localization, had for standard deviation $\sigma = 4$ cm in x and y, and $\sigma = 2$ cm in z. We see that the improvement is really significant with only one additional encoder wheel.

References

[1] G. Bayer *et al.* Leitdrahtlose navigation von baumaschinen. In *Proceedings of the third International Symposium on Road Construction Systems and Technologies*, Munich, Germany, Apr. 1998.

[2] S. Booth. Surveying and construction machine control systems. *Engineering Surveying Showcase, Royal Institution of Chartered Surveyors*, 1:42–46, 1999.

[3] B. Gorham. Method and apparatus for determining position. UK Patent GB 2090096B, Oct. 1979.

[4] B. Gorham. A novel method of digital height transfer using a laser. In *Proc. Commission VI, International Federation of Surveyors (FIG), 16th International Congress*, Montreux, France, June 1981.

[5] B. Gorham. A new technique of position fixing for site vehicles. In *Proceedings of the 13th International Symposium on Automation and Robotics in Construction*, pages 717–727, Tokyo, Japan, June 1996.

[6] J.-F. Le Corre and F. Peyret. SIREM: the absolute location of civil-engineering equipment. *Mechatronic Systems Engineering*, 1:183–192, 1990.

[7] P. S. Maybeck. *Stochastic Models, Estimation and Control*, volume 141–1, page 366. Academic Press, 1979.

[8] L. Pampagnin, F. Peyret, and G. Garcia. Architecture of a GPS-based guiding system for road compaction. In *Proceedings of the 1998 IEEE International Conference on Robotics and Automation*, pages 2422–2427, Leuven, Belgium, May 1998.

[9] F. Peyret. A new facility for testing accurate positioning systems for road construction robotics. *Automation in Construction*, 8(2):209–221, Dec. 1998.

[10] F. Peyret, D. Bétaille, and G. Hintzy. High-precision application of GPS in the field of real-time equipment positioning. In *Proceedings of the 14th International Symposium on Automation and Robotics in Construction*, pages 2–10, Pittsburgh, Pennsylvania, USA, June 1997.

[11] F. Peyret, J. Jurasz, A. Carrel, E. Zekri, and B. J. Gorham. The computer integrated road construction project. *Automation in Construction*, 2000. To be published.